Power Over Fiber System for Heterogeneous Sensors Multiplexing

Armando Rodriguez, Evelyn Vanegas-Tenezaca, Jose R. Vento Alvarez, Manuel Lopez-Amo, *Senior Member, IEEE*, and Mikel Bravo

***Abstract*—This paper presents a Power-over-Fiber based remote electronic and optical fiber sensors multiplexing scheme. The system architecture consists of a 50-km linear cavity Raman-fiber laser that is used for interrogation of FBG optical fiber sensors. Simultaneously, electronic sensors information is modulated in amplitude while the optical sensors' data are encoded in the spectral information. In order to bias the electronic sensors, the residual power of the Raman pump laser is collected in an energy harvesting unit. This electric power is used for biasing an ATTiny85 control unit and two electro-optical modulators. A proof-of-concept is presented where a couple of optical fiber-Bragg-gratings sensors collect strain information that is self-compensated in temperature according to the digital data achieved from the electronic sensors. A 9.6 kbit/s data rate was achieved using Mach-Zehnder amplitude modulators and a maximum 35 *ksample/s* was retrieved using a high-speed C-band spectrometer and performing spectral analysis via a software developed in Python.**

***Index Terms*—Energy harvesting, fiber Bragg grating, modulator, multiplexing, power over fiber.**

I. Introduction

THE role of optical fiber technology has become nothing short of transformative thanks to as remarkable features as the immunity to electromagnetic interference and many chemicals, high bandwidth, its flexibility and a low transmission loss over long distances, among others. Beyond their pivotal role in telecommunications, optical fibers have found applications as optical sensors, pointing out the small sizes at which they can be manufactured. It is also remarkable their inert behavior in hostile environments, where conventional electronic sensor cannot properly operate.

The transmitting fiber's light-guiding properties may be altered by a specific parameter of interest to be measured, such as temperature, strain, pressure, chemical species. Thus, the fiber serves as both the transmission medium and the sensing element.

In addition, optical fiber sensing technology can be significantly extended by exploring new system architectures to multiplex sensors and by implementing new technological mechanisms [1]. This has allowed to combine several sensors of different nature in the same fiber, either punctual or distributed ones. A scaled fiber sensor network structure which operation mode is based on a fiber ring laser which combines Raman and Erbium doped fiber amplification was experimentally demonstrated in [2].

A key advancement in this field is the remote power supply of electro-optical devices using optical fibers. This feature enables for immediate monitoring and prompt action, and eliminates the logistical hassle of providing electrical power to remote places [3].

It is well known that one solution that has provided new opportunities for the creation of complex and remotely powered networks is the so-called "Power over Fiber (PoF)" technology [4], [5]. PoF has being introduced into a wide variety of applications with the aim of remotely power supplying and interrogating sensor networks [6], [7], [8], [9], [10].

To utilize long distance PoF-based sensors systems, a good alternative is the use of photocells biased at 1445 nm wavelength. At this wavelength, nowadays most of fibers show low-loss performance, and the remote PoF systems can cover up to 100 km. At this distance a remote switch can be biased, as was demonstrated in [11]. There, the power supplied by a Raman laser pump was employed. A Remote PoF-biased switching TDM Brillouin Optical Time Domain Analysis distributed sensor multiplexing structure was deployed in [12]. Moreover, a fully-switchable fiber laser based on random distributed feedback for optical sensors (fiber Bragg grating and intensity-based sensors) interrogation was designed and tested in [13]. All these

Manuscript received 15 March 2024; revised 27 May 2024 and 6 June 2024; accepted 8 June 2024. Date of publication 12 June 2024; date of current version 16 September 2024. This work was supported in part by MCIN/AEI/10.13039/501100011033 and FEDER "A way to make Europe," under Project PID2022-137269OB-C21, in part by MCIN/AEI/10.13039/501100011033 and European Union "Next generation EU"/PRTR under Project TED2021-130378B-C22, and in part by MICINN under the Beatriz Galindo BEAGAL18/00116 Grant. Open access funding provided by Universidad Publica de Navarra. *(Corresponding author: Armando Rodriguez.)*

Armando Rodriguez and Manuel Lopez-Amo are with the Electrical, Electronic and Communication Engineering Department and Institute of Smart Cities (ISC), Universidad Publica de Navarra, 31006 Pamplona, Spain (e-mail: armando.rodriguez@unavarra.es; mla@unavarra.es).

Evelyn Vanegas-Tenezaca is with the Electrical, Electronic and Communication Engineering Department, Universidad Publica de Navarra, 31006 Pamplona, Spain (e-mail: evelyndayanara.vanegas@unavarra.es).

Jose R. Vento Alvarez is with the Telecommunication and Electronic Engineering Department, Universidad de Pinar del Río, Pinar del Río 20100, Cuba, and also with the Electrical, Electronic and Communication Engineering Department, Universidad Publica de Navarra, 31006 Pamplona, Spain (e-mail: joseraul.vento@unavarra.es).

Mikel Bravo is with the Electrical, Electronic and Communication Engineering Department and Institute of Smart Cities (ISC), Universidad Publica de Navarra, 31006 Pamplona, Spain, and also with the MendiTech, Sensores de Fibra Optica, 31006 Pamplona, Spain (e-mail: mikel.bravo@unavarra.es).

Color versions of one or more figures in this article are available at https://doi.org/10.1109/JLT.2024.3413582.

Digital Object Identifier 10.1109/JLT.2024.3413582

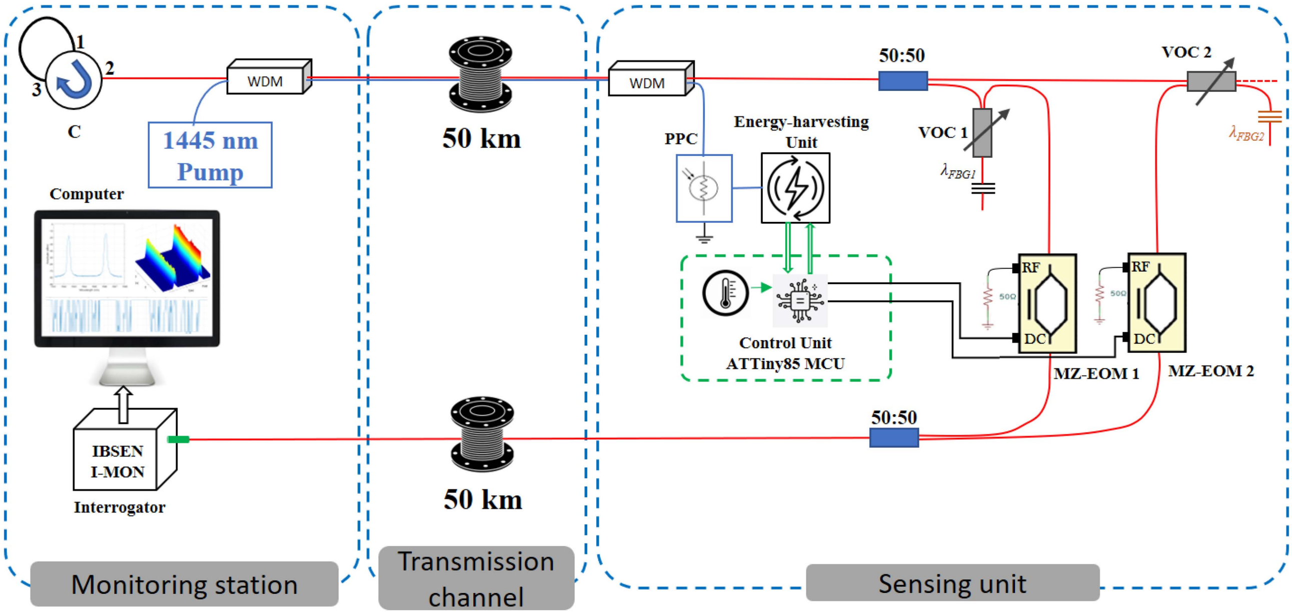

Fig. 1. Experimental setup of the 50-km PoF based multiplexed system. Upper fiber: Raman fiber laser. Lower fiber: passive collecting fiber. (C: Circulator; WDM: Wavelength Division Multiplexer; PPC: Photovoltaic Power Converter; VOC: Variable Optical Coupler; MZ-EOM: Mach-Zehnder Electro-Optical Modulator).

applications used low power MEMS devices to reduce the energy consumption.

Furthermore, energy harvesting (EH) is the process of capturing and converting ambient forms of energy from the surrounding environment into usable electrical power [14]. Since the 90´s of last century, several studies have been conducted to improve the PoF efficiency using new EH systems [9], [15], [16], [17].

The combination of several types of sensors in the same network have been in the research interest in the last years. A multiplexed system for both electronic and optical fiber sensors was discussed in [18]. The authors developed a 10-km interrogation system based in PoF were the data from an array of FBGs are modulated in amplitude to encode the data from an electronic sensor.

In this work, we present an enhanced multiplexing mechanism to interrogate a 50-km remote hybrid sensors network that is power supplied using a PoF architecture. We propose a modulation scheme to simultaneously transmit the electronic sensor data encoded in the optical amplitude of the spectrum while transmitting the wavelength shift information. We designed and implemented a configuration to interrogate several optical sensors independently, each of them with different digital encoded data, using a high-frequency measurement and detection methods. Moreover, we integrate an EH system to take full advantage of the energy transmission resources over long distances.

II. Experimental Setup

The experimental setup for the proposed system is depicted in Fig. 1. At the monitoring station, the high-power light source is a Raman pump semiconductor-based laser IPG *Fibertech* RLD-3D-1445. It operates at 1445 nm which provides Raman amplification pump for signal level stabilization and laser generation on C-band, moreover, it is used to power supply the electronic components and sensors in the sensing unit subsystem [19]. A circulator in the seed signal branch acts as a mirror to close one end of the linear cavity to generate the laser. This is possible because of two FBG sensors, one of them at 1542.4 nm and the other at 1546 nm, which act as wavelength-selective mirrors.

The wavelength division multiplexer (WDM) combines the pump and the reflected signal in the circulator and transmitted along a 50-km single-mode fiber (SMF) segment. Such fiber, manufactured by Corning, conforms to the ITU-T G.652 recommendation, with a core diameter of ~9 μm and the mode field diameter (MFD) is 10.5 μm, which represents an effective area of 86.6 μm^2. This optical fiber has a maximum attenuation of 0.17 dB/km at 1550 nm, giving a Raman-gain effective length of ~20 km for the length of fiber being used. For these features, the Raman-gain coefficient is 6×10^{-14} m/W at 1550 nm [20].

In the other end, at sensing unit, other WDM separates both the laser seed light and the 1445-nm Raman pump. The pump light is converted in electric energy via a *JDSU* PPC-9LW photocell that is able to achieve a power efficiency of 35% at 100 mW at a wavelength of 1445 nm, with up to 4 V and 8.75 mA output ratings. Thus, the PPC output is connected to an EH controller to exploit the energy resources and to accumulate in a capacitor pool.

A 3 dB optical coupler splits the laser light into two sensing branches. Each branch has an FBG sensor used to strain measurements. Because these sensors are sensitive to strain and temperature simultaneously, a temperature compensation is needed while measuring strain. Fig. 2 describes the temperature characterization of the FBG sensors used in the experiment, showing a sensitivity of 9.965 pm/°C and 9.99 pm/°C, respectively.

The reflection of the sensors is coupled back with two 905(P)-M variable optical couplers from *Evanescent Optics* that are used to set the optimal coupling ratio, thus their respective spectral

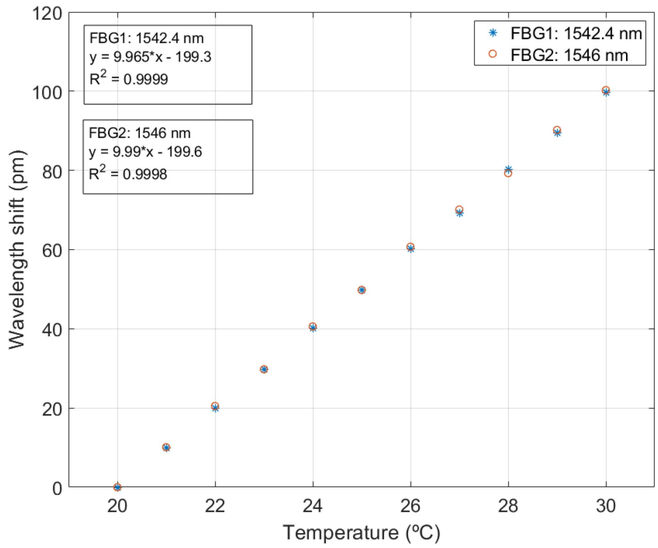

Fig. 2. Temperature characterization of the FBG sensors.

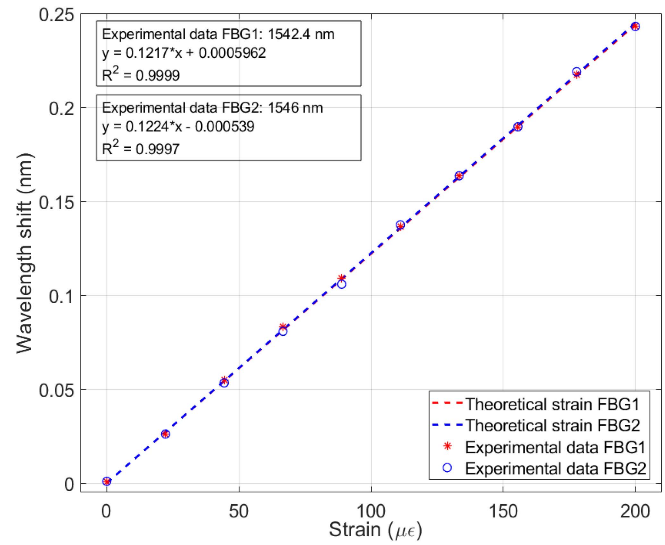

Fig. 3. Strain characterization of the FBG sensors.

response be similar in amplitude. The experimental power data measured show a coupling ratio of 60.6%:39.4%. Secondly, they are connected to two independent Mach-Zehnder electro-optical amplitude modulators (MZ-EOM). The first one is an AVANEX 20-AM modulator which has a bias voltage (V_π) of 5 V at 1 kHz, the electrical drive voltage is 4 V and an optical extinction ratio of 20 dB. The second one is a UTP APE 2 × 2-1.5-1.0-1-1-C modulator that have an input impedance > 1 kΩ, the $V_\pi < 2.5$ V and a typical extinction ratio of 22 dB at 1550 nm. Finally, the outputs of the modulators are coupled in another 3 dB optical coupler and transmitted to the monitoring station via a secondary 50-km optical fiber path.

These devices have a strong polarization dependence because they incorporate annealed proton exchange (APE) polarizing waveguides in which only the TE mode is allowed to propagate. For this reason, the use of highly depolarized light sources, such as the generated Raman laser, helps to mitigate this effect in the modulators.

The FBG sensors were characterized also to strain sensitivity. As was discussed in [21], the strain is dependent in the FBG wavelength and can be calculated by:

$$\Delta\lambda/\lambda \;=\; 0.79\,\Delta L/L \qquad (1)$$

The theoretical strain sensitivities of the sensors are 1.22 pm/με for the FBG_1 and 1.224 pm/με on the case of FBG_2. Furthermore, an experimental analysis was performed, where both FBGs, with a 10-mm grating length, are stressed up to 200 με in a micro-positioning-controlled platform. Fig. 3 depicts the results of strain characterization showing a good agreement with the theoretical data.

The harvester unit is an AEM30940 driver from *e-Peas*. This is a highly-efficient, regulated dual-output, integrated energy management circuit that harvests the available input current up to 110 mA. It integrates an ultra-low power boost converter to charge a storage element, such as a Li-ion battery, a thin film battery, a supercapacitor or a conventional capacitor. It incorporates two voltage outputs; the low-voltage (LVOUT) supply with a selectable voltage of 1.2 V or 1.8 V, up to 20 mA and the high-voltage (HVOUT) supply with at a configurable voltage between 1.8 V to 4.1 V, up to 80 mA. Both are driven by highly-efficient LDO (Low DropOut) regulators for low noise and high stability. For this setup, the LVOUT was set at 1.8V and the HVOUT at 4V, while the storage element is a 32-mF capacitor.

The control unit is an 8-bit *ATTiny85* microcontroller (MCU) from Microchip, that is able to operate in a range of 2.7 V to 5.5 V and low power consumption of 540 μW at 1.8 V and 1 MHz internal clock in active mode. The power ratings meet the specification of the EH unit. As a proof of concept, an AD22103K temperature sensor is used to compensate the strain measurements on FBGs. This sensor provides an analog voltage output according to a temperature coefficient of 28 mV/°C. The operating voltage is from 3.3 V to 5 V. On the other hand, a water lever data from the SEN0204 sensor (*DFRobot*) is also used to modulate the wavelength amplitude of the second FBG. This sensor operates between 3.8 V and 24 V and the current consumption is 5 mA, with a response time of 500 ms. In Fig. 4 is depicted the schematics of circuitry of the control unit.

The harvester driver is able to start operating at an input voltage as low as 380 mV and an input power of just 3 μW. Then, it enables the LVOUT providing power supply to the MCU which is checking the capacitor charge process via STATUS pin. Once the storage element has charged over 2.2 V, then a flag indicator rises and the MCU enables the HVOUT via HV_EN pin. This feature is used to power on the high-consumption devices such as a water lever sensor and the electronic temperature sensor. Then, it retrieves the sensor status and finally, power-off the sensor back.

The data from the electronic sensors are encoded by the MCU in a serial data frame at 9600 bauds. The temperature information is modulated in the FBG_1 wavelength amplitude, connecting the serial transmission pin to the DC port in the modulator. This port

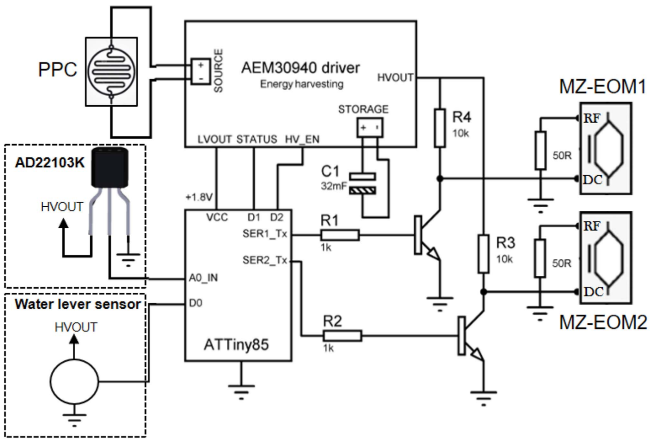

Fig. 4. Control unit and energy harvesting driver schematics.

has a high input impedance, which, added to the low frequencies of the modulating signal, facilitates the coupling of the MCU serial bus and makes it optimal for modulating the optical signal. In case of the water level sensor, the information is modulated in the FBG_2 wavelength amplitude. Both modulators are driven by NPN transistors in voltage-follower setup as signal level adapter for the electrical drive input.

At the monitoring station, the spectra are retrieved via an FBG interrogator IBSEN I-MON 256 HS. This instrument consists of a spectrometer with a detection wavelength range from 1525 nm to 1570 nm, providing a maximum resolution < 0.5 pm and a measurement frequency up to 35 kHz. A customized Python software was developed to read the raw data from interrogator via the Ethernet interface and to process the spectral information.

III. Results and Discussion

The experiment was carried out by generating the laser signal in the upper 50-km optical fiber linear cavity. The experimental setup was developed in an air-conditioned room with constant temperature of 23 °C. The Raman-based laser was characterized performing a gradual increase of the laser driver current and measuring the output power. Fig. 5 depicts the characterization results. The pump power started at 0.2 W and the laser generation occurs around 1.6 W. The peak power of the FBG wavelength increased up to −42.02 dBm and −41.62 dBm, respectively. The inset figure depicts the spectral response of the generated laser at 1.75 W for a 0.03-nm resolution in the optical spectrum analyzer, where a linewidth of 0.14 nm and 0.16 nm was observed, respectively. The total received power at the monitoring station was −23.7 dBm.

The spectrum is retrieved by an IBSEN I-MON interrogator as was mentioned before. The custom-made software in Python open a TCP socket connection via Ethernet and send configuration commands to set the detection parameters. Firstly, the I-MON was configured to measure the spectra at 35 *ksample/s*, using an exposure time of 1.408 µs, a clock divider of 22 which gives a detector clock of 10.417 MHz. Finally, a command starts the measurement and the spectrometer send the raw spectral data via an UDP socket, thus the software is

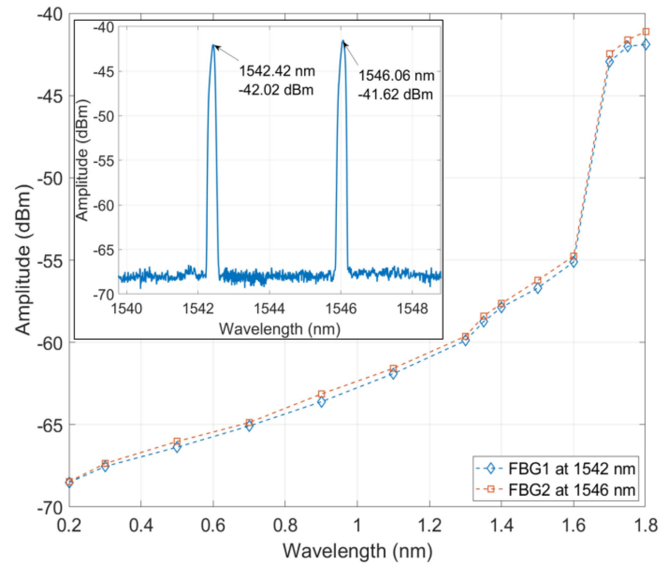

Fig. 5. Raman-based laser characterization. *Inset:* Laser spectrum at 1.75 W pump.

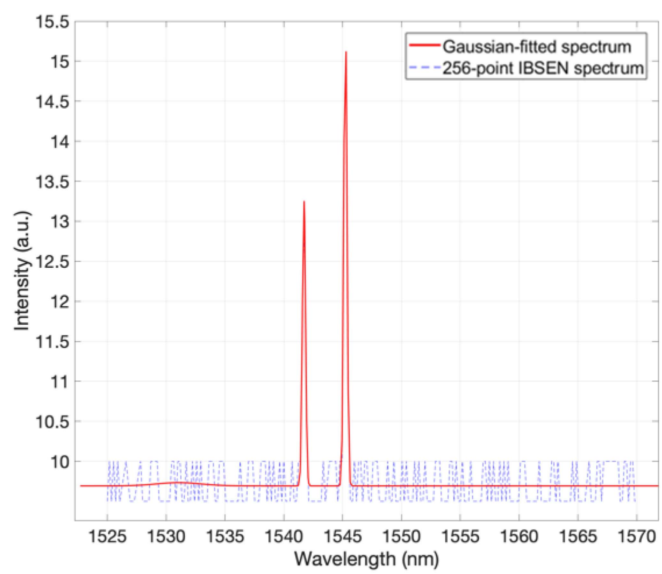

Fig. 6. 256-point spectrum retrieved from IBSEN I-MON interrogator and Gaussian-fitted curve of the spectrum.

designed to simultaneously listen for incoming packets. Each packet contains 553 bytes of information, of which 512 bytes are from the sensor data. This payload structure represents a 2-byte frame for each of 256 pixels of the spectrometric analysis.

For this reason, the raw data are a low-resolution representation of the spectral response. To enhance the peak wavelength detection and shift, the software performs a mechanism to fit the obtained curve. A Gaussian-fit method is implemented using 4 terms and a *Trust-region* algorithm, giving a total of 12 coefficients [22]. In addition, the fitted curve is interpolated on 45000 points, thus the wavelength resolution is increased up to 1 pm. Moreover, the received spectral data in raw format and the fitted curve is saved into a file. Fig. 6 depicts a received

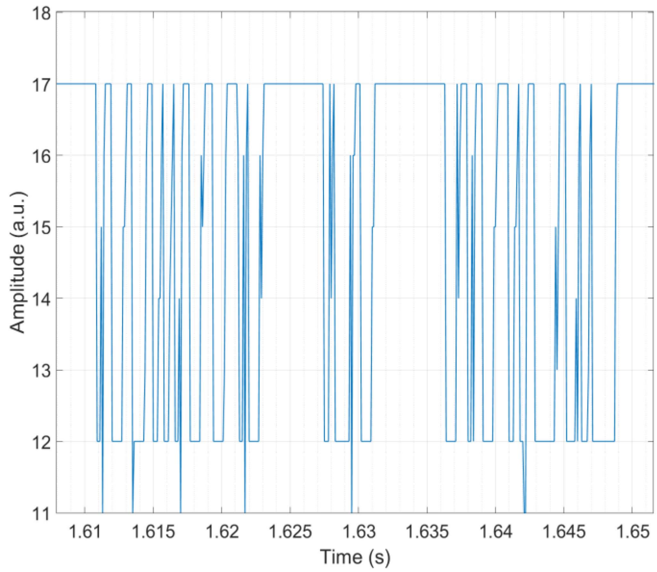

Fig. 7. Serial data frame decoded from FBG_1 wavelength peak tracking.

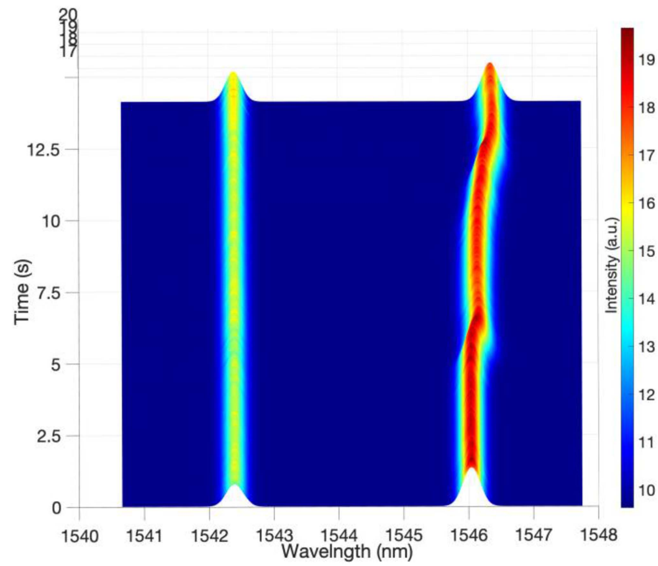

Fig. 8. Spectral representation of the wavelength evolution of FBG sensors during the experiment.

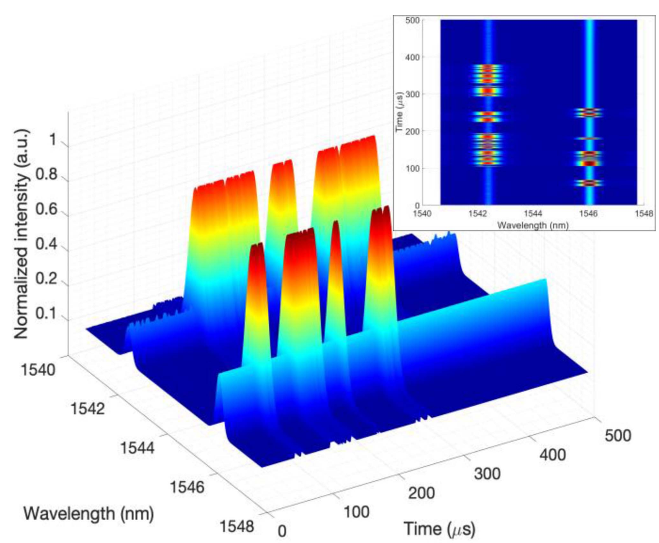

Fig. 9. Serial data encoded in the wavelength amplitude of FBG sensors. *Inset:* Top view.

sample of the fiber optical sensors, in dashed blue line the raw spectrum obtained with I-MON and in solid red line, the fitted curve according to Gaussian model. The intensity is expressed in arbitrary units (a.u.).

The FBG peak wavelength can be further tracked and decoded as the electronic sensor data are modulated in the amplitude. In the program, a code snippet calculates the wavelength peak of every received spectrum data from I-MON, setting as detection threshold over 12 a.u. in amplitude, hence the maximum value is considered. Each wavelength peak is associated with its spectral position because its value is expected to decrease below the threshold or disappear, due to modulation. With this strategy, the variation of the wavelength of each sensor and its amplitude are recorded.

As a result, Fig. 7 shows a section of the evolution of the FBG_1 peak wavelength during the experimental time, representing the digital frame waveform. A sample of 15 seconds of measurement has been taken and then zoomed to the time interval where the data frame has been transmitted. The serial data parameters are the standard 9.6 *kbit/s*, with 8 data bits and 1 stop bit. The decoded information shows the temperature measured by the AD22103K sensor at the time of experimental test, which was 23.14 °C.

The spectral evolution of the two FBG sensors along the experiment is depicted in Fig. 8. As demonstration, the FBG_1 was positioned in such a way to avoid wavelength variation due to stress. The FBG_2 was forced to a step increase of stress up to 240 $\mu\varepsilon$ using a micro-positioning platform. Consequently, the wavelength shift registered was 290 pm.

In addition, an enlarged view of the spectral evolution shows the data frame pattern encoded in the wavelength amplitude. Fig. 9 depicts in perspective a section of the experimental data acquired, also, in the inset figure, shows a top view of the encoded information. The left-side graphics correspond to data frame of temperature and on the right side the water level status data.

In terms of energy consumption, the control unit required a total power of 25.2 mW. Table I presents a detailed summary of the measured consumption for each device. The current measurements were performed with a *Promax* PD-163 multimeter. The MCU showed a higher power consumption compared to the technical specifications, being about 2.1 mW. This represents the time of maximum processing tasks of the microcontroller, when both serial ports are transmitting data to the modulators and the MCU reading information from the temperature and water level sensors, simultaneously.

The scalability of the system can be approached from several perspectives. As placing more optical sensors means using passive components that add losses. According to the work developed by [23], in a WDM-architecture where the transmission fiber segment is amplified and using 10% coupling ratio optical

TABLE I
ENERGY REQUIREMENTS OF THE CONTROL UNIT

Device	Theoretical current consumption (mA)	Measured power consumption (mW)
ATTiny 85 MCU	0.3	2.07
AD22103K (temperature sensor)	0.5	1.5
SEN0204 (Water level sensor)	5	17.9
AVANEX 20-AM (MZ-EOM)	0	0
Transistor-based signal level stages	1.07	3.73
Total	**6.87**	**25.2**

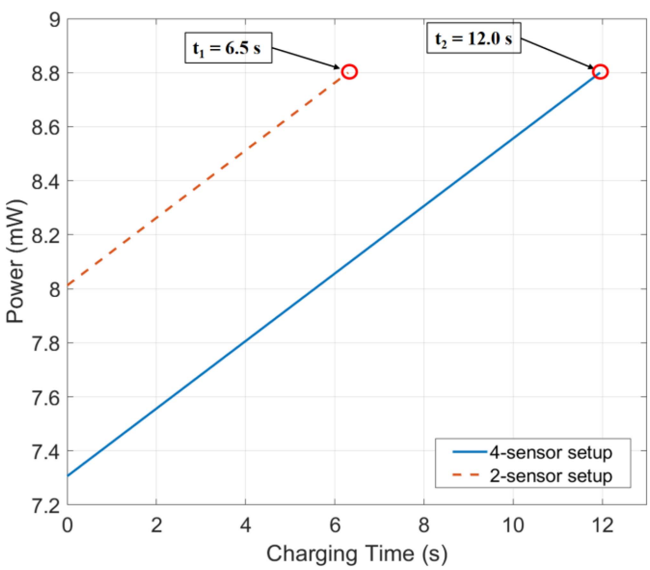

Fig. 10. Effect of electric load in the time of capacitor charge process.

couplers, and the reception segment acts as passive fiber path with 5% coupling ratio optical couplers, it is possible to escalate up to 30 different sensors.

In the proposed system, e.g., using four sensors instead of two, an identical number of electronic sensors are needed to encode their information on the optical carrier. This would increase energy consumption as the load resistance is higher, impacting the charge recovery rate of the storage element in the harvesting controller. Therefore, the delay time between transmitted frames is increased, as well. Fig. 10 describes the process of resuming capacitor charge after disabling the electronic sensors, reading the information and transmitting the modulated signal for the 2-sensor and 4-sensor systems. The charging recovery time for the 32-mF capacitor pool increases up to 12 s, due the additional sensors as the load increases.

Regarding the optical sensors scalability, in the work developed in [18], a broad-band source was used as seed signal that is transmitted along 10 km of SMF fiber and the whole FBG sensor array is modulated. In this work, a remote network has been demonstrated, wherein the transmission channel is utilized as a laser cavity, and the residual pumping power is harnessed to power electrical sensors or other desired components. Two FBGs have been employed for laser feedback, simultaneously serving as sensors and optical information carriers. The information is modulated onto the FBGs using remotely powered modulators. Additionally, a high-speed spectrometer has been utilized to track the FBG spectral lines and extract the encoded information within a single device. An alternative to scalability is to create a hybrid solution that combines both studies.

IV. CONCLUSION

In conclusion, the key novelty and focus of this work are the demonstration of a power-over-fiber based multiplexing architecture that can simultaneously interrogate both optical FBG-based sensors and electronic sensors over the same 50-km fiber link. The system uses the residual pump power for energy harvesting to remotely power the electronic components and modulators. We have leveraged existing multiplexing techniques like wavelength encoding for the FBGs and amplitude modulation for the electronic sensors, in conjunction with the power-over-fiber architecture.

A Raman-based pump of 1.75 W was used to power-supply the electronic devices and to stimulate the laser generation to interrogate the optical sensors and to be the carrier of the electrical sensor data. In addition, an energy harvesting system has been implemented to exploit the energy resources of the optoelectrical conversion stage in combination with low-power control devices. The energy demand does not exceed 10% of the harvester's storage and distribution capacity.

The digital data from the electronic sensors were modulated in amplitude and, afterwards coded using the wavelength of two FBG sensors via two Mach-Zehnder modulators. The encoded data were transmitted at 9.6 *kbit/s*, while the spectral data of the FBGs were retrieved at 35 *ksample/s* using a high-speed FBG sensor interrogator and optimized software decoding methods. The FBG sensors measured the strain variation, and the ambient temperature data measured with an electronic sensor were transmitted simultaneously to compensate for the thermal effect in the strain measurement. The performance metrics like the electronic sensor data rate, FBG sampling rate, and strain/temperature resolutions are described with the aim to establish a proof-of-concept implementation of the hybrid multiplexed sensing approach that is fully driven by optical power delivery over fiber.

The study offers the possibility of further scalability of the system, multiplexing more optical sensors and commercial low-power electronic sensors.

Conflicts of Interest: The authors declare no conflict of interest.

REFERENCES

[1] R. A. Perez-Herrera and M. Lopez-Amo, "Fiber optic sensor networks," *Opt. Fiber Technol.*, vol. 19, no. 6, pp. 689–699, Dec. 2013, doi: 10.1016/j.yofte.2013.07.014.

[2] M. Bravo, M. Fernández-Vallejo, M. Echapare, M. López-Amo, J. Kobelke, and K. Schuster, "Multiplexing of six micro-displacement suspended-core Sagnac interferometer sensors with a Raman-Erbium fiber laser," *Opt. Exp.*, vol. 21, no. 3, Feb. 2013, Art. no. 2971, doi: 10.1364/OE.21.002971.

[3] J. D. Lopez-Cardona, C. Vazquez, D. S. Montero, and P. C. Lallana, “Remote optical powering using fiber optics in hazardous environments,” *J. Lightw. Technol.*, vol. 36, no. 3, pp. 748–754, Feb. 2018, doi: 10.1109/JLT.2017.2776399.

[4] B. C. DeLoach, R. C. Miller, and S. Kaufman, “Sound alerter powered over an optical fiber,” *Bell System Tech. J.*, vol. 57, no. 9, pp. 3309–3316, Nov. 1978, doi: 10.1002/j.1538-7305.1978.tb02205.x.

[5] R. C. Miller and R. B. Lawry, “Optically powered speech communication over a fiber lightguide,” *Bell System Tech. J.*, vol. 58, no. 7, pp. 1735–1741, Sep. 1979, doi: 10.1002/j.1538-7305.1979.tb02280.x.

[6] M. Matsuura, “Recent advancement in power-over-fiber technologies,” *Photonics*, vol. 8, no. 8, Aug. 2021, Art. no. 335, doi: 10.3390/photonics8080335.

[7] E. P. Putra et al., “Technology update on patent and development trend of power over fiber: A critical review and future prospects,” *J. Photon. Energy*, vol. 13, no. 1, Jan. 2023, Art. no. 011001, doi: 10.1117/1.JPE.13.011001.

[8] M. Fernandez-Vallejo, S. Rota-Rodrigo, and M. Lopez-Amo, “Remote (250 km) fiber Bragg grating multiplexing system,” *Sensors*, vol. 11, no. 9, pp. 8711–8720, Sep. 2011, doi: 10.3390/s110908711.

[9] R. Peña, C. Algora, I. R. Matías, and M. López-Amo, “Fiber-based 205-mW (27% efficiency) power-delivery system for an all-fiber network with optoelectronic sensor units,” *Appl. Opt.*, vol. 38, no. 12, Apr. 1999, Art. no. 2463, doi: 10.1364/AO.38.002463.

[10] C. Budelmann, “Opto-electronic sensor network powered over fiber for harsh industrial applications,” *IEEE Trans. Ind. Electron.*, vol. 65, no. 2, pp. 1170–1177, Feb. 2018, doi: 10.1109/TIE.2017.2733479.

[11] M. Bravo, M. A. Erro, J. M. Algueta, S. Diaz, and M. Lopez-Amo, “Remote fiber optic switch powered by light for robust interrogation of fiber Bragg grating sensor networks,” *Meas. Sci. Technol.*, vol. 24, no. 9, Sep. 2013, Art. no. 094021, doi: 10.1088/0957-0233/24/9/094021.

[12] M. Bravo, A. Ullan, A. Zornoza, A. Loayssa, M. Lopez-Amo, and J. Lopez-Higuera, “Application of remote power-by-light switching in a simplified BOTDA sensor network,” *Sensors*, vol. 13, no. 12, pp. 17434–17444, Dec. 2013, doi: 10.3390/s131217434.

[13] M. Bravo, V. De Miguel Soto, A. Ortigosa, and M. Lopez-Amo, “Fully switchable multi-wavelength fiber lasers based on random distributed feedback for sensors interrogation,” *J. Lightw. Technol.*, vol. 33, no. 12, pp. 2598–2604, Jun. 2015, doi: 10.1109/JLT.2015.2397191.

[14] A. Harb, “Energy harvesting: State-of-the-art,” *Renewable Energy*, vol. 36, no. 10, pp. 2641–2654, Oct. 2011, doi: 10.1016/j.renene.2010.06.014.

[15] Y. Li, Z. Xiao, Z. Zhang, and L. Li, “A novel remote multi-sensing energy management system based on power-over-fiber transmission,” in *Proc. IEEE 4th Int. Conf. Energy, Elect. Power Eng.*, 2021, pp. 125–129, doi: 10.1109/CEEPE51765.2021.9475697.

[16] A. Lopez-Martin, J. M. Algueta, and I. R. Matías, “Energy harvesting approaches in IoT scenarios with very low ambient energy,” *Renewable Energy Power Qual. J.*, vol. 17, pp. 183–187, Jul. 2019, doi: 10.24084/repqj17.257.

[17] J. C. Casaleiro, “On the feasibility of GPON fiber light energy harvesting for the Internet of Things,” *Eng., Environ. Sci., Comput. Sci.*, vol. 4, no. 1, 2018, Art. no. 254620.

[18] A. Rodriguez-Rodriguez, E. Venegas-Tenezaca, M. Bravo, and M. Lopez-Amo, “Remote interrogation of a versatile and hybrid sensors network using power over fiber,” in *Proc. 28th Int. Conf. Opt. Fiber Sensors*, 2023, Paper W4.99, doi: 10.1364/OFS.2023.W4.99.

[19] M. Bravo, A. Ullan, A. Zornoza, A. Loayssa, M. Lopez-Amo, and J. Lopez-Higuera, “Application of remote power-by-light switching in a simplified BOTDA sensor network,” *Sensors*, vol. 13, no. 12, pp. 17434–17444, Dec. 2013, doi: 10.3390/s131217434.

[20] G. P. Agrawal, *Fiber-optic Communication Systems*, 5th ed. Hoboken, NJ, USA: Wiley, 2022.

[21] C. Campanella, A. Cuccovillo, C. Campanella, A. Yurt, and V. Passaro, “Fibre Bragg grating based strain sensors: Review of technology and applications,” *Sensors*, vol. 18, no. 9, Sep. 2018, Art. no. 3115, doi: 10.3390/s18093115.

[22] H. Guo, “A simple algorithm for fitting a Gaussian function,” in *Streamlining Digital Signal Processing*, 1st ed., R. G. Lyons Ed. Hoboken, NJ, USA: Wiley, 2012, pp. 297–305. doi: 10.1002/9781118316948.ch31.

[23] R. Hernandez-Lorenzo, M. Lopez-Amo, and P. Urquhart, “Single and double distributed optical Amplifier fiber bus networks with wavelength division multiplexing for photonic sensors,” *J. Lightw. Technol.*, vol. 16, no. 4, pp. 485–489, Apr. 1998.

Armando Rodriguez received the Telecommunication and Electronics Engineering degree from Universidad de Pinar del Río, Pinar del Río, Cuba, in 2017. He has been an Instructor with Telecommunication and Electronics Department, Universidad de Pinar del Río, since 2017. He has been a member of Postgraduate School of Education organized by VLIR-UOS Cooperation Project of Belgium and Universidad de las Ciencias Informáticas, Havana, Cuba, since 2019. He is currently a Predoctoral Researcher and Member of Institute of Smart Cities, Universidad Pública de Navarra, Pamplona, Spain. His research interests include fiber-optic sensors, microstructured optical fibers, fiber Bragg gratings, power-over-fiber based systems, and energy harvesting systems.

Evelyn Vanegas-Tenezaca received the Engineering degree in telecommunications technologies from the Universidad Pública de Navarra, Pamplona, Spain, in 2022. She is currently working toward the master’s degree in telecommunications engineering with the Universidad Pública de Navarra. She is also a Project Assistant with the Universidad Pública de Navarra in the research project “TED2021-130378B-C22”. Her research interests include fiber-optic sensors, hollow core fibers, micro-fibers, and optical interrogation.

Jose R. Vento Alvarez received the Engineering degree in telecommunications from the Instituto Politécnico de Tecnología de la Habana, Havana, Cuba, in 1982, and the M.S. and Ph.D. degrees in telecommunications engineering from University Politécnica de Madrid, Madrid, Spain, in 1996 and 1998, respectively. Since 1990, he has been a Professor of data transmission, optical communications, networking and telecommunications systems with the Telecommunication Department, University of Pinar del Rio, Pinar del Río, Cuba. He has developed researching activities with Photonic Technology Department, Polytechnic University of Madrid, Madrid related with Advanced optical system communications, in 2008, 2009, 2012, 2023, respectively. During 2005–2007 was a Visiting Assistant Professor with the State University of Mato Grosso, Caceres, Brazil, and was a Visiting Researcher with the School of Computing, Engineering and Information Sciences, North Umbria University, Newcastle upon Tyne, U.K, in 2011. Since 2017, he has been a Visiting Professor with the Universidad Pública de Navarra, Pamplona, Spain,. His research interests include optical fiber sensors, protocols engineering and Smart Cities, topics on which he has supervised several theses and coauthored both journals and conference papers.

Manuel Lopez-Amo (Senior Member, IEEE) has been a Full Professor of photonics with the Electrical and Electronic Department, Universidad Pública de Navarra, Pamplona, Spain, since 1996. He is the Head of the Optical Communications Group, Electrical and Electronic Department, Universidad Pública de Navarra. He is the Chairman of the Optoelectronic Committee of Spain. He is the Director of the Engineering Faculty and of the Electrical and Electronic Department, Universidad Pública de Navarra. He is the leader of more than 60 research projects. He has supervised 18 PhD theses about photonics. He has authored or coauthored more than 400 works in international refereed journals and conferences related with fiber-optic networks, fiber-optic sensors, fiber-optic amplifiers and lasers and integrated optics. He is the Spanish representative at the experts committee IEC SC86C WG2 on Fiber Optic Sensors. He is a Member of the technical committees of the International Conference on fiber optic sensors (OFS) and the European Workshop on optical fiber sensors (EWOFS), among others.

Mikel Bravo received the Telecommunication Technical Engineering, Communications degree, and the master’s and Ph.D. degrees from the Universidad Pública de Navarra, Pamplona, Spain, in 2007, 2010, and 2015, respectively. In 2008, he joined the Optical Communications Group and, after a postdoctoral stay in the University of Sherbrooke, he returned to UPNA as researcher. In 2021, he Co-Founded the spin-off company MendiTech. He is currently a Researcher with the Electrical, Electronic and Communications Department and a Member of the Smart Cities Institute, Universidad Pública de Navarra, Pamplona, Spain, and is the Director of Menditech, Sensores de Fibra Óptica S.L., Pamplona. His research interests include structural health monitoring, fiber Bragg gratings, interferometric sensors, multiplexing architectures, optical amplifiers, and optical networks.